

BENEFITS OF PRECISION SCHEDULING AND SPACING FOR ARRIVAL OPERATIONS

Shannon Zelinski, NASA Ames Research Center, Moffett Field, CA

Abstract

Advances in arrival scheduling and controller aids for spacing have potential benefits of reducing aircraft delays and increasing airport arrival throughput. Schedulers use fixed arrival paths to estimate aircraft time-to-fly and assign them arrival slots based on the required separation plus a buffer. Concepts that reduce arrival time uncertainty can take advantage of advanced scheduling with smaller spacing buffers. These concepts have been successfully demonstrated with a handful of near to mid-term traffic demand scenarios and technologies using spacing buffers as low as 0.3 nmi. The analysis published here characterizes the observed arrival spacing behavior of 29 runways belonging to 15 airports within 8 of the busiest terminal areas across the United States for 32-60 days worth of traffic. The typical observed instrument arrival buffers ranging from 0.5 to 1.5 nmi would equate to roughly 10-20% increase in runway arrival capacity if buffers were reduced to 0.3 nmi. The effect of fixed arrival routing on terminal area flight time was also studied. Most runways studied had significant path stretch delay. This work estimates that 1-2 min of this delay could be reduced with precision scheduling and most of the remainder could be absorbed by speed control.

Introduction

Advances in arrival scheduling and spacing have potential benefits of reducing aircraft delays and increasing airport arrival throughput. Schedulers use fixed arrival paths to estimate aircraft time-to-fly and assign them arrival slots. The size of an arrival slot is based on the required separation between leading and trailing aircraft plus a buffer used to mitigate arrival time uncertainty and reduce the probability of a separation violation. Thipphavong and Mulfinger [1] showed that delay and throughput benefits are more sensitive to these spacing buffers than the uncertainty itself. But the appropriate spacing buffer to achieve a desired controller intervention rate does decrease significantly with the uncertainty, allowing more

benefit. To this end, benefit analyses have focused on showing the arrival time accuracy achievable for a specific technology or concept of operations employing a set of technologies [2-7]. The larger benefit of the increased accuracy is unclear.

Some studies have extrapolated or measured the benefit of scheduling and spacing precision on delay and throughput as compared to current day operations. The Terminal Area Precision Scheduling and Spacing System [8-9] verified in human-in-the-loop simulations that precision scheduling and spacing tools can allow spacing buffers of 0.3-0.4 nmi to accommodate 10-15% more traffic than current operations. However, the results are limited to a handful of simulated 100-minute traffic scenarios for a single airport. Ballin and Erzberger [10] analyzed the arrival spacing precision for 30 Dallas Fort Worth (DFW) rush periods and estimated that a 0.25 nmi separation buffer should allow for at least 15% more capacity than was observed. Again, this analysis focused on a single airport and since then, DFW operations have changed considerably.

In addition to allowing reduced spacing buffers, precision scheduling and spacing concepts use defined fixed arrival paths such as Area Navigation (RNAV) and Required Navigation Performance (RNP) routing to achieve full benefit. Economic and environmental benefits (fuel usage and noise) of RNP have been quantified in case studies [11-12]. The broader impact of fixed arrival routing and reduced separation buffers and the variability of this impact between different terminal areas are unclear.

This paper characterizes the observed arrival spacing behavior of 29 runways belonging to 15 airports within 8 of the busiest terminal areas across the US for 32-60 days worth of traffic. Potential capacity increases due to reducing the observed 0.5 to 1.5 nmi spacing buffers to 0.3 nmi are estimated. Then fixed arrival paths are designed for each runway. The impact of these fixed paths and reduced buffers on average flight arrival time is then estimated.

Method

Arrival flights to multiple airport runways from multiple terminal areas were analyzed to encompass a wide range of traffic arrival environments, from metroplexes to super-hubs, across the National Airspace System (NAS). The traffic analysis was performed using recorded Terminal Radar Approach Control (TRACON) flight plan and track data. First, separation behavior was characterized for each airport runway. Theoretical runway arrival capacities were estimated based on observed current spacing behavior and expected spacing behavior afforded by precision scheduling and spacing concepts. This study also estimated the effect precision scheduling and spacing along fixed arrival routes would have on terminal area flight time. RNAV arrival routes were designed to each runway and new scheduled arrival times were compared with historical arrival times using historical aircraft arrival paths.

Scope of Study

Flight plan and track data from the eight busiest TRACON facilities in the NAS (Atlanta, Chicago, Denver, Dallas/Fort Worth, New York, Potomac, Northern California, and Southern California) were examined. The data covered between 32 and 60 24-hour traffic samples distributed between February 2010 and early May 2010. Traffic samples were required to have uninterrupted TRACON track data between 0600 and 2200 local time. These same data were used in two previous studies where data statistics are described in more detail [13-14].

This analysis focused on airport runways with relatively large numbers of tightly spaced instrument arrival operations. These included 29 runways from 14 of the 29 NPIAS (National Plan of Integrated Airport Systems [15]) identified large hubs and one satellite airport (TEB) diagrammed in Figure 1. Locations of satellite airports for which track data was available but were not included in this analysis are also shown.

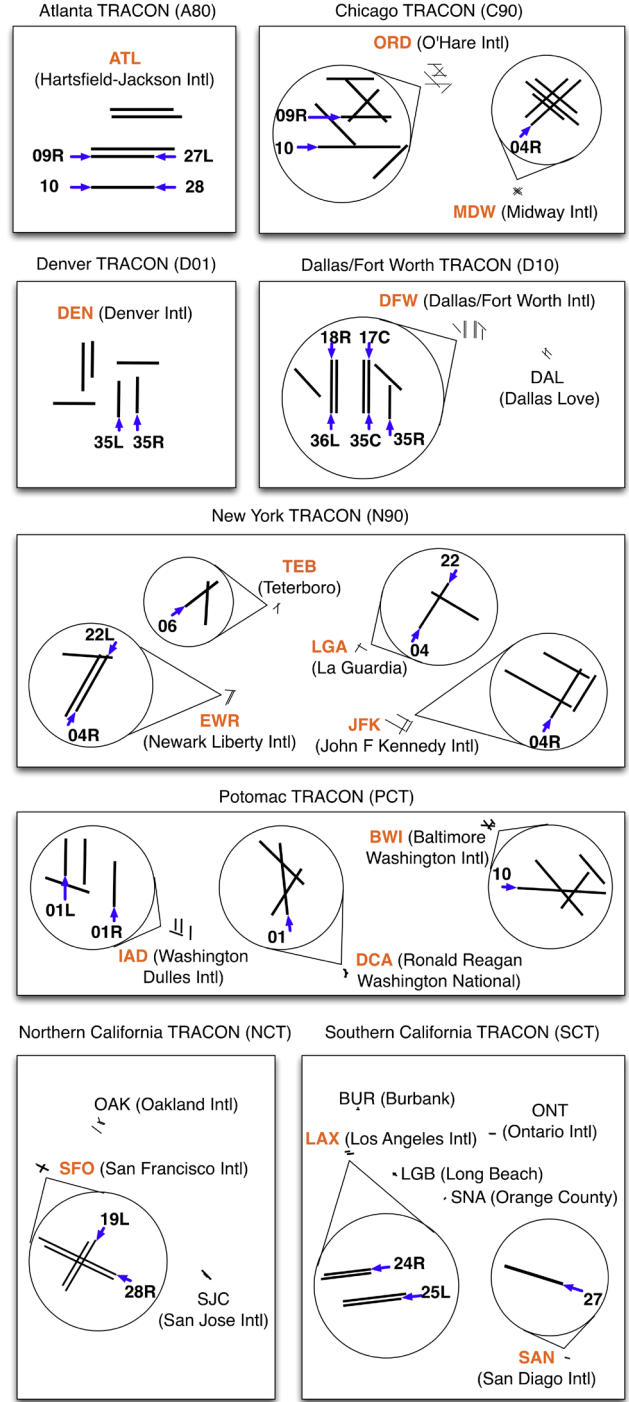


Figure 1. Runway Diagrams

Separation Behavior from Track Data

To characterize the unique separation behavior of each runway, Ballin and Erzberger's [10] method was modified to accommodate samples outside rush periods and differentiate between behavior observed

during Visual Approach Conditions (VAC) and Instrument Approach Conditions (IAC). Robinson and Kamgarpour [13] describe the method used to determine each aircraft's landing runway and threshold crossing time from the track data. For each sequential pair of aircraft landing at the same runway, the position of the trailing aircraft at the time the leading aircraft crossed the runway threshold was extrapolated from the two track points on either side of this time. The observed separation was then calculated as the trailer's along-path distance from this point to the runway threshold.

Sequential aircraft pairs to the same runway were segregated by their minimum in-trail separation requirements (standard radar separation [16-17]) determined by leader/trailer weight class. Table 1 shows the leader/trailer weight class to required separation mapping in nmi. For pairs requiring 3 nmi separation, in-trail separation at the runway threshold can be reduced to 2.5 nmi under certain conditions [16]. However, these conditions were not considered in this analysis.

Table 1. Minimum Required Separation

		Trailer				
		Super	Heavy	B757	Large	Small
Leader	Super	6	6	8	8	10
	Heavy	4	4	5	5	6
	B757	4	4	4	4	5
	Large	3	3	3	3	4
	Small	3	3	3	3	3

Aircraft pairs with the same separation requirement were further segregated between VAC and IAC according to the airport's weather conditions during the quarter hour in which the trailer landed. The FAA's Aviation System Performance Metrics (ASPM [18]) data provide VAC and IAC state in quarter hour intervals. VAC and IAC separation histograms were generated with a 0.1 nmi separation bin size. Figure 2 shows an example separation histogram for characterizing separation behavior.

Then a +/-3-sigma Gaussian kernel smoother with a 2 nmi span was used to smooth each histogram. The maximum bin of the smoothed histogram within a -1 to +5 nmi range of the required separation standard was assumed to be the observed target separation s . The curves generally followed the two-part separation model convolving a normal distribution of the positioning accuracy of the controller/pilot team with a Poisson distribution of the arrival gaps. The Poisson distribution can be large due to low demand periods, which can shift the mean far to the right of the maximum. Therefore, the standard deviation σ from s was calculated using only observed separations (not the smoothed curve) less than or equal to s . This is shown as an arrow pointing to the left of the target separation in Figure 2. Let r be the minimum required separation. The separation buffer b was then $s-r$. These separation behavior metrics were calculated the same way for VAC and IAC. The subscripts VAC and IAC differentiate metrics by weather condition in the results section.

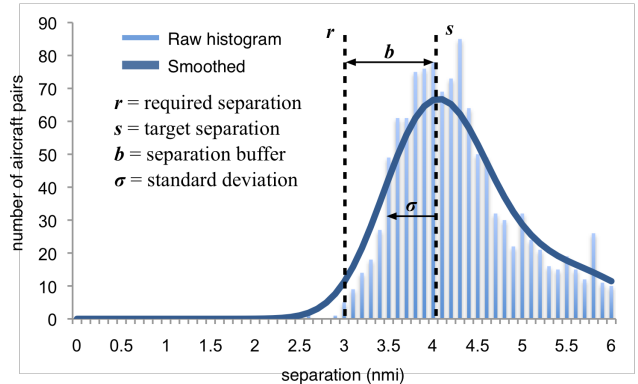


Figure 2. Example Separation Histogram

A final behavior metric, safety margin, was calculated as $x=b/\sigma$. It was designed as a simple proxy for separation conformance. Let n_s be the number of separations less than or equal to s and let n_r be the number of separations less than r . The empirical separation conformance is given by $c_e=1-(n_r/n_s)$, that is the ratio of observed separations to the left of s that conform to the required separation minimum r . The analytical probability of separation conformance is given by the Gauss error function $c_a=\text{erf}(x/\sqrt{2})$. Assuming that the curve to the left of s has a normal distribution, c_a was expected to be similar to c_e . With this simplification, if 95% conformance was required to be considered safe, then

x would need to be at least 2. Values of x below 2 would quickly fall out of acceptable conformance.

The above metrics require a significant number of high arrival rate operations to generate a meaningful characterization. The 29 runway subset

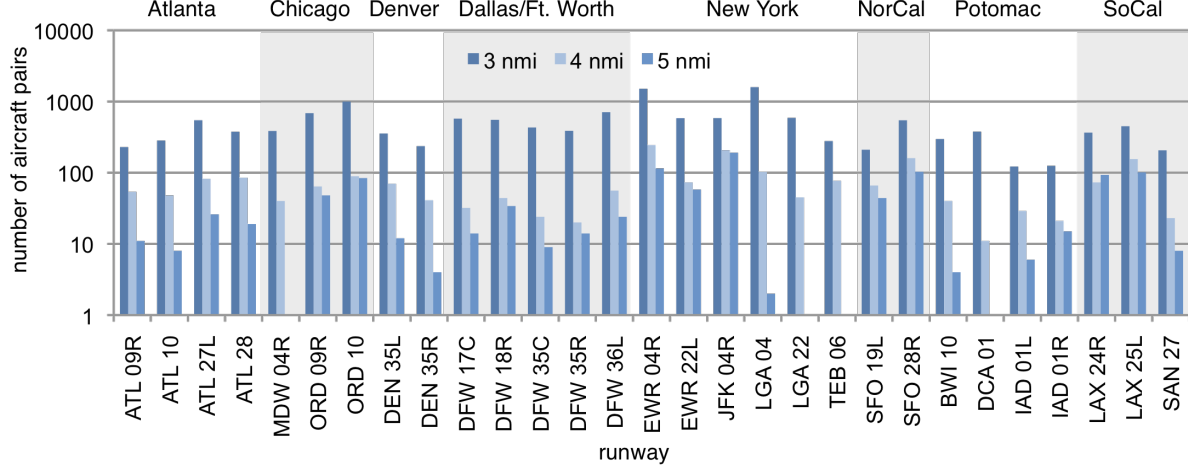


Figure 3. Number of Instrument Arrival Separations $\leq s$ (n_s)

The most frequent required separation at any runway is 3 nmi, with much fewer instances as the separation requirement increases. This is due to a preponderance aircraft of large weight class. The number of instances for required separations greater than 5 nmi were less than 10 at all but two runways at $r=6$ nmi and so are not shown in Figure 3. Of the runways shown, 8 have fewer than 9 instances for $r=5$ nmi and the separation histograms were too sparse to represent a normal distribution. For the remaining 21 runways for $r=5$ nmi, and all 29 runways for $r=3$ or 4 nmi, the arrival separations less than or equal to s have a fairly normal distribution as demonstrated by how similar the analytical separation conformance is to the empirical separation conformance in Figure 4. Figure 4 shows the differences between empirical c_e and analytical c_a separation conformance by required separation.

On average the empirical ratio of separations conforming to the required minimum is higher than the analytical probability by just 0.02 (on a 0 to 1 scale). Therefore, the distributions are fairly normal and the safety metric x is a good proxy for separation conformance.

These separation behavior metrics were calculated the same way for VAC and IAC. The

for this analysis was chosen for their relatively high values of n_s in IAC. Figure 3 shows the IAC n_s at each of these runways for required separations of 3, 4, and 5 nmi. The numbers of aircraft pairs are shown on a logarithmic scale.

subscripts VAC and IAC are used to differentiate metrics by weather condition in the results section.

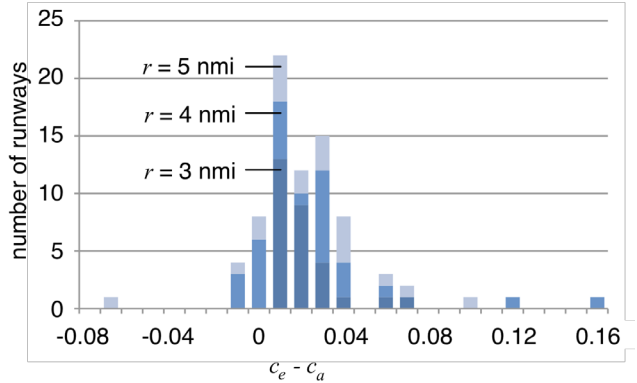


Figure 4. Separation Conformance Comparison

Runway Arrival Capacity

Runway arrival capacity is the estimated number of arrival slots that can be scheduled to a runway within a given amount of time. Average slot size can vary depending on the typical landing speeds and mix of aircraft weight class at each runway, as well as the spacing buffer used. For each aircraft, the desired spacing with its leading aircraft is computed as the required separation plus a given buffer. The time at which the aircraft reaches this along path distance

from the runway threshold is calculated by interpolating between track points on either side of this along-path distance. This desired spacing time is then subtracted from the runway threshold crossing time to get the scheduling slot size for the flight. The average slot size for each runway is then divided into 15 minutes to get a quarter hourly arrival capacity.

Fixed Routing and Path Stretch Delay

Precision scheduling concepts require fixed arrival routes such as RNAV and RNP but very few arrival routes have been defined all the way to the runway in today's system. Therefore, fixed arrival routes to each runway studied were designed for the purposes of this analysis. Most RNAV/RNP procedures designed in practice overlay existing routes to avoid lengthy environmental reviews [19]. Fixed arrival routes for this study were designed to follow the nominal flow of arrival traffic. A graph-based trajectory bundling algorithm [20] was used to identify the most consistently used paths to each runway. Separate routes were generated for turboprops and jets where it was clear their nominal paths deviated significantly. In some cases the resulting routes curved unnecessarily in places due to consistently used path stretch maneuvers and these route segments were smoothed out manually.

A flight was assigned on a fixed route to its arrival runway at the track point that first came within 3 nmi of the fixed route. From this point, the flight was directed to the next downstream waypoint along the route and then followed the route to the runway. The flight was expected to follow a deceleration profile similar to that of its original trajectory as it followed the fixed route. To model this assumption, first the original flight track was segmented using the closest track point to each fixed route waypoint. Original flight track segments were then mapped to fixed route segments using these closest points. Figure 5 illustrates the path stretch delay calculation for a sequence of mapped closest flight track and fixed route points labeled 1 through 5. Let p_{ij} and q_{ij} be mapped original flight track (orange) and fixed route segments (green) respectively. Let $t(p_{ij})$ and $t(q_{ij})$ be the respective times to travel each segment, and let $l(p_{ij})$ and $l(q_{ij})$ be the respective lengths of each segment. Then $t(q_{ij})=t(p_{ij})l(q_{ij})/l(p_{ij})$. The sum of the differences in flight time ($t(p_{ij})-t(q_{ij})$) across each mapped segment

is the path stretch delay d . Note that path stretch delay may be negative if the original flight path is sufficiently shorter than the fixed route.

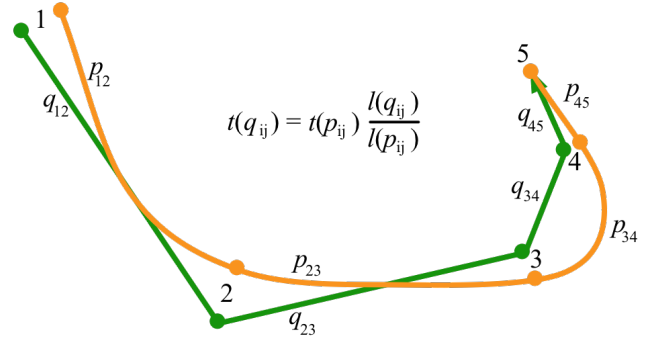


Figure 5. Example Path Stretch Delay Calculation

Fixed Route Scheduling and Time Saved

To determine the effect of fixed routing and scheduling buffers on terminal area delay, flights were rescheduled according to their fixed route Estimated Time of Arrival (ETA). The fixed route ETA was calculated as Observed Time of Arrival (OTA) minus the path stretch delay. The flights were then re-sequenced according to their fixed route ETAs, and delay was applied as Scheduled Time of Arrival (STA) assigned to place flights within arrival slots appropriately sized to meet the required separation with respect to the leading aircraft plus a given buffer. The time saved or reduced path stretch delay by using the fixed path and given buffer is then OTA-STA. Note that time saved cannot exceed path stretch delay. The time saved is somewhat conservative because flights with path stretch delay may have been slowed as well and the path stretch delay calculation does not compensate for this, but assumes a similar speed profile to the original flight trajectory.

Results

Separation Behavior by Required Separation

Quartiles for IAC and VAC separation buffers, standard deviations, and safety margins by required separation are shown in Figure 6 as box and whisker plots. From top to bottom the box and whisker

divisions represent max, 75%, 50%, 25%, and min values for each set of data. The quartiles for the 3 and 4 nmi required separations represent all 29 runways.

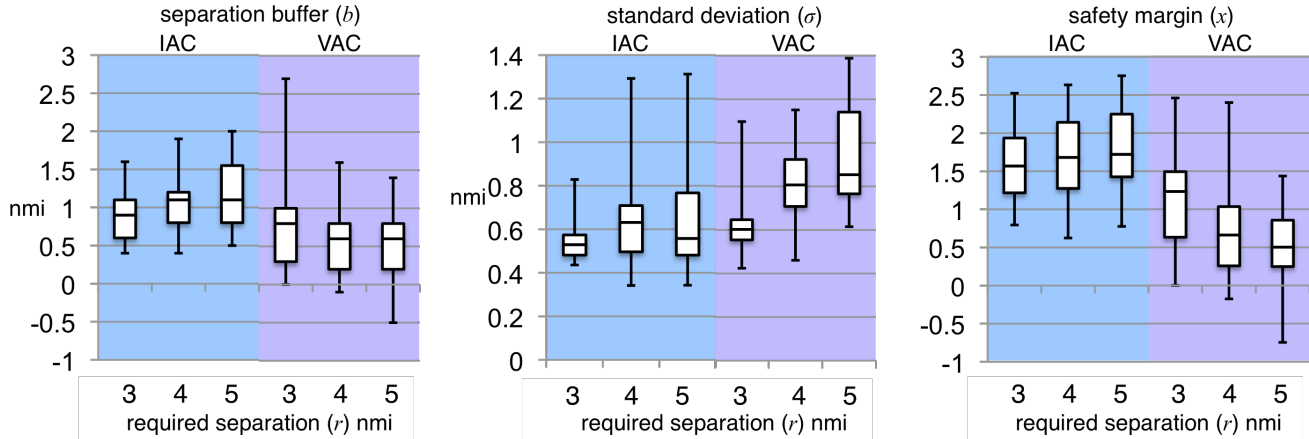


Figure 6. Separation Metrics by Required Separation

The mean IAC separation buffer is approximately 1 nmi with an increasing trend as required separation increases. This additional buffer compensates for the increasing IAC standard deviation. It even tends to overcompensate as can be seen by the increasing IAC safety margin. VAC standard deviation also increases with required separation but it tends to be higher than IAC standard deviation. This means that a single target separation is less often accurately achieved under VAC.

Unlike the IAC, VAC buffers remain fairly stable as standard deviation increases so there is no compensation. Under IAC, buffers are never below 0.4 mi, whereas the VAC buffers can be negative. This means that the VAC target separation can be below the IAC required separation.

Even though the VAC safety margin is quite low and decreases as required separation increases, this does not mean that these operations are unsafe. The VAC safety margin is calculated with respect to IAC requirements and so this metric merely shows how different the separation behavior is between IAC and VAC.

Separation Behavior by Runway

Individual separation behavior by runway is compared for 3 nmi required separation as most aircraft pairs fall in this category. Figure 7 shows separation behavior metrics for each individual runway for 3 mi required separation. The blue and

The quartiles for 5 nmi required separation represent only the 21 runways for which IAC n_s was at least 9.

purple columns represent IAC and VAC target separation (s) respectively, with single tail standard deviation (σ) whiskers. The 3 nmi required separation (r) is highlighted in yellow so that the part of the target separation columns protruding above can be visualized as the buffer. The IAC safety margins (x) are shown as red diamonds to visualize runways' need to reduce standard deviation or freedom to reduce buffers relative to each other.

In general, runways within the same TRACON tend to behave similarly. DEN and SFO runways have the largest x_{IAC} because they have the smallest IAC standard deviations but among the largest separation buffers. They may benefit from advanced scheduling that reduces the buffers. DFW also has fairly high spacing buffers but they are scaled appropriately to their standard deviations. DFW's x values between 1.7 and 2.0 equate to c_a probabilities between 0.92 and 0.95, which is quite reasonable. More precision would enable DFW to further reduce its separation buffers. Airports in the remaining TRACONS, particularly LGA and IAD are not using separation buffers that sufficiently compensate for their standard deviations. The significant benefit of increased precision at these heavily strained airports may be to reduce controller workload and separation violations. By contrast, the two runways with the largest IAC buffers and standard deviations, TEB 06 and SAN 27, have the lowest arrival traffic volume among the runways analyzed within their TRACONS.

They may be neglected due to higher priority airports

nearby.

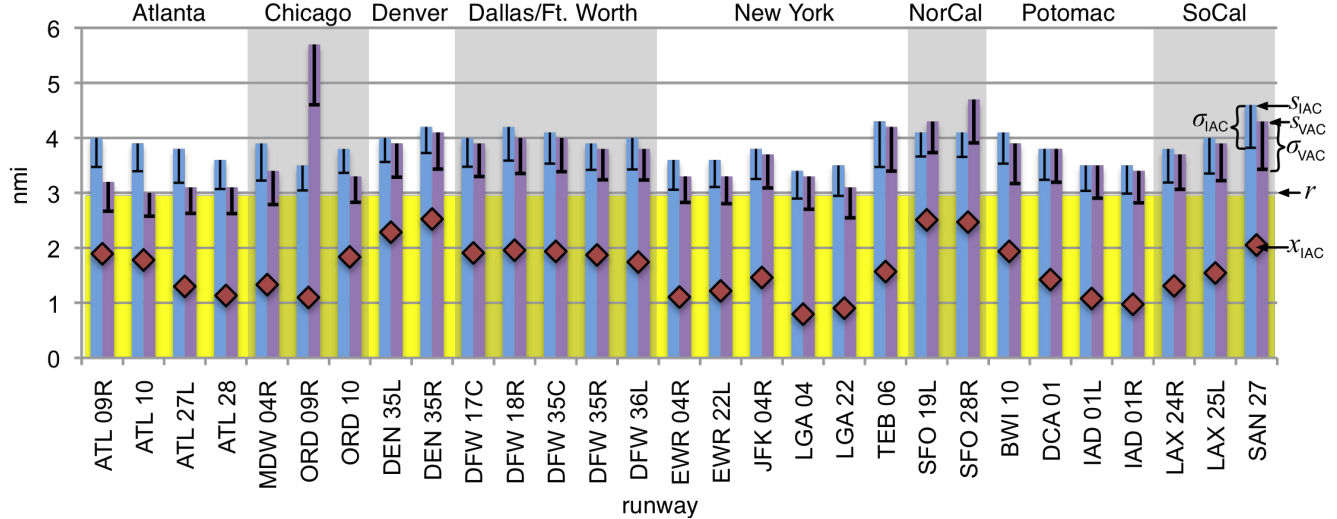


Figure 7. Separation Metrics by Runway

In general, IAC target separations are larger than VAC. The difference between IAC and VAC is negligible for DEN, DFW, JFK, DCA, IAD, and LAX, suggesting that advanced scheduling would provide similar benefits under both IAC and VAC. In contrast, ATL has much lower target separations in VAC than IAC and so very little if any benefit would be gained during VAC using IAC separation requirements. All four ATL runways analyzed can use 2.5 nmi separation which was not considered, so their actual buffer may be 0.5 nmi larger.

Only three runways analyzed (ORD 09R, SFO 19L and 28R) have VAC target separations that are larger than IAC. This may be due to procedural constraints. ORD 09R handles arrivals and departures most of the time. However, it may be used mostly for arrivals in IAC. Figure 8 shows smoothed VAC and IAC spacing histograms for ORD 09R. Assuming the shape of the VAC curve is due to normal shared arrival/departure operations, the IAC curve appears to be a convolution of dedicated arrival operations and shared arrival/departure operations. The lighter blue curves show a possible deconvolution of IAC where 0.35VAC (the VAC curve multiplied by 0.35) represents the shared arrival/departure behavior and the remainder (IAC-(0.35VAC)) represents the dedicated arrival behavior.

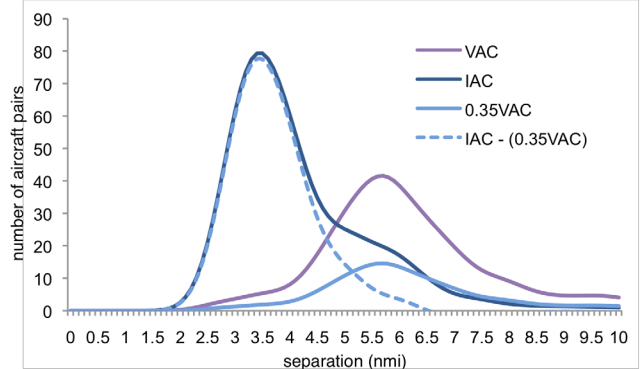


Figure 8. ORD 09R Spacing Behavior

SFO has two sets of closely spaced parallel runways that perform simultaneous arrivals in VAC but 19L and 28R perform single arrivals in IAC. Figure 9 shows smoothed arrival spacing histograms for SFO 28L and 28R separately and together (28LR). Individually, 28R and 28L receive a large number of arrivals in VAC. In IAC, 28R accepts the vast majority of arrivals. When the runways are analyzed together (28LR), a single peak appears for IAC but two peaks appear for VAC. The first peak represents coupled aircraft performing simultaneous operations and the second peak represents the spacing between sets of simultaneous operations. The histograms for 19R and 19L show a similar but less pronounced effect.

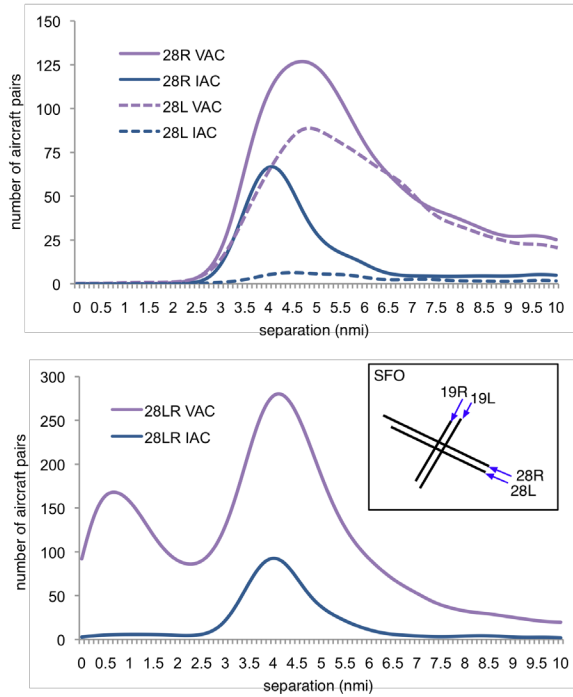


Figure 9. SFO 28L and 28R Spacing Behavior

Runway Arrival Capacity Estimates

Swenson et al [8] successfully demonstrated safe IAC operations within a simulation of LAX using a 0.4 nmi scheduled buffer and recent tests of the same

concept simulating Dallas Love Field (DAL) arrivals have used 0.3 nmi scheduling buffers. Figure 10 shows estimated quarter hour capacity for each runway using scheduling buffers of b_{VAC} , b_{IAC} , or 0.3 nmi. The percent change in 0.3 nmi buffer capacity from the estimated VAC and IAC capacity is also shown.

Given that the observed IAC buffers are between 0.4 and 2 nmi as seen in Figure 7, it is not surprising that 0.3 nmi buffers are estimated to increase IAC capacity up to 30%. ATL VAC buffers are so low that using 0.3 nmi buffers would actually reduce capacity based on 3 nmi rather than 2.5 nmi required separation. Although VAC buffers and capacity estimates tend to be lower than IAC, many of the VAC buffers are above 0.3 nmi, resulting in estimated capacity increases around 20%. Many of these runways such as TEB may lack sufficient demand to achieve these theoretical capacities or they are affected by other constraints such as shared arrival/departure operations or crossing runway restrictions. Other airports such as EWR, LGA, and IAD show an increase over IAC capacity with little to no change in VAC capacity, which suggests that demand is not lacking and that with precision spacing, it may be possible to achieve VAC throughput under IAC.

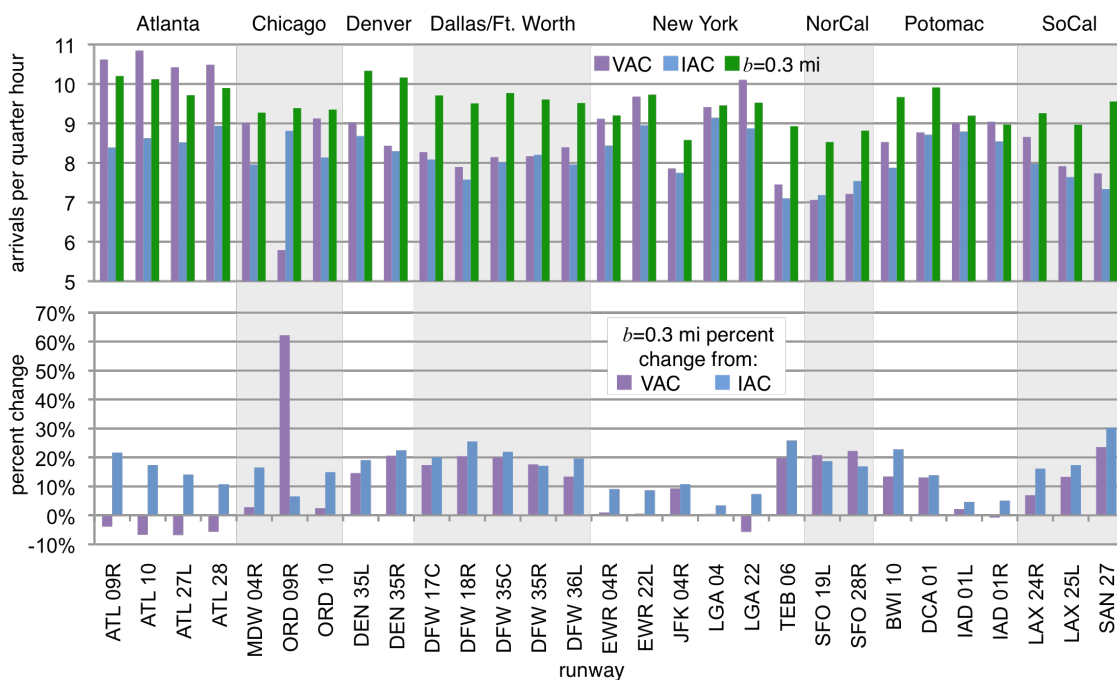


Figure 10. Estimated Arrival Capacity

Path Stretch Delay and Time Saved by Runway

Each flight was assigned to the first fixed route that came within 3 nmi of its original track, which was used to calculate the flight's path stretch delay and fixed route ETA. Flights were sequenced according to fixed route ETA and assigned scheduled arrival slots using spacing buffers ranging between 0 and 1.0 nmi in 0.1 nmi increments. Figure 11 shows the 5% trimmed mean path stretch delays and time saved for the range of scheduling buffers. The 5% trimmed mean is used rather than the pure mean to filter the effects of a few large outliers such as undetected go-arounds and other processing errors. The black rectangles mark the 5% trimmed mean path stretch delays for each runway. The 5% trimmed mean time saved results are represented by blue rectangles with width proportional to the buffer used. The 0.3 nmi buffer results for each runway are highlighted in green as this buffer size has been successfully tested in simulations of DAL arrival operations.

As expected, time saved is inversely proportional to the buffer size. Some runways tend to be more sensitive to buffer size than others as can be

seen in Figure 11 by the rapidly decreasing time saved results as the buffer size increases from 0 to 1.0 nmi. Runways at ATL, ORD, EWR, and LGA are particularly sensitive to buffer size. These runways have tightly packed schedules with visual arrivals often spaced closer than the minimum required spacing for instrument arrivals. Therefore, any increase in spacing buffer quickly compounds delay as each delay is shared by each flight in the tightly packed stream. Runways TEB 06 and SAN 27 are least sensitive to buffer size because both their IAC and VAC observed buffers were larger than 1.0 nmi, the upper range of buffer size tested.

Figure 12 shows smoothed histograms of the time saved results for two runways with different sensitivity to buffer size. LGA 22 is very sensitive to buffer size, which can be seen in Figure 12 as the histograms shift to the left with increasing buffer size. In contrast, DEN 35R is less sensitive to buffer size with time saved results very similar to the path stretch delay. DEN 35R is also the runway with the most clearly visible histogram multi modality due to different amounts of typical path stretch time each flight can save, depending on which fixed path they follow.

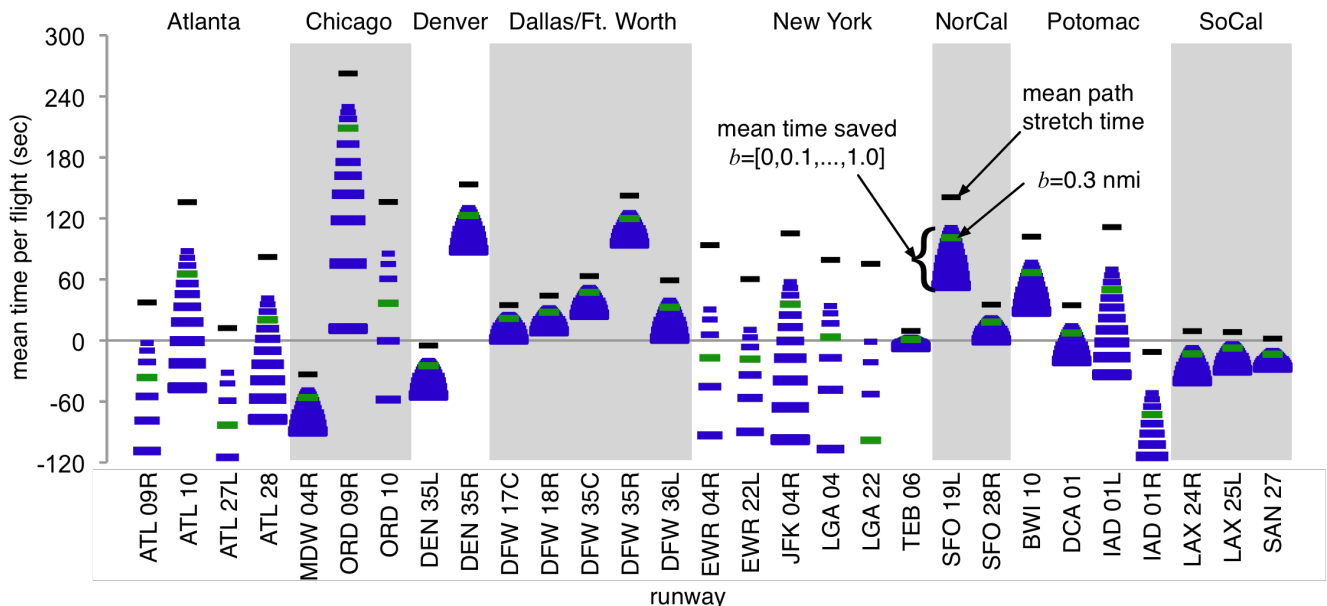


Figure 11. Path Stretch Delay and Time Saved by Runway

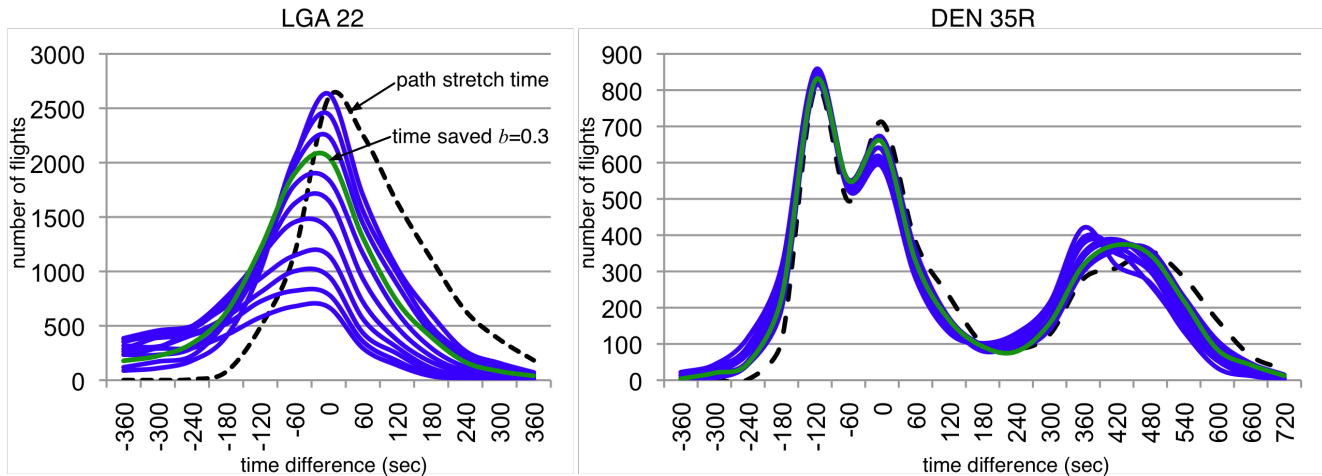


Figure 12. LGA 22 and DEN 35R Time Saved Histograms

As can be seen in Figure 11 most runways have a positive path stretch delay. That is, in general, more flights are given a path stretch than a short cut relative to the fixed arrival routing identified. Figure 13 shows the flight tracks and fixed routing for the runways with lowest (MDW 04R) and highest (ORD 09L) path stretch delay. The dotted lines represent the lateral paths of historical tracks color-coded by path stretch delay relative to the fixed routing represented by the blue nodes and links. The green tracks are at least 2 minutes shorter than the fixed route and the red tracks are at least 4 minutes longer than the fixed route. Even though the fixed routing for MDW 04R is consistent with published RNAV instrument approach procedures for that runway, most flights from the East take shorter paths, perhaps due to visual approaches. Relatively few flights with more than 4 minutes of path stretch delay can be seen holding from the West or performing a base turn from the East. However, ORD 09L has a large amount of path stretch delay. Holding patterns and S-turns can be seen near all the major entry points. But the main contributor to path stretch delay is a large extended base turn to the West of the runway. Traffic from all directions is affected by this inefficiency, even traffic from the West, which doubles back on itself to merge with the extended base turn.

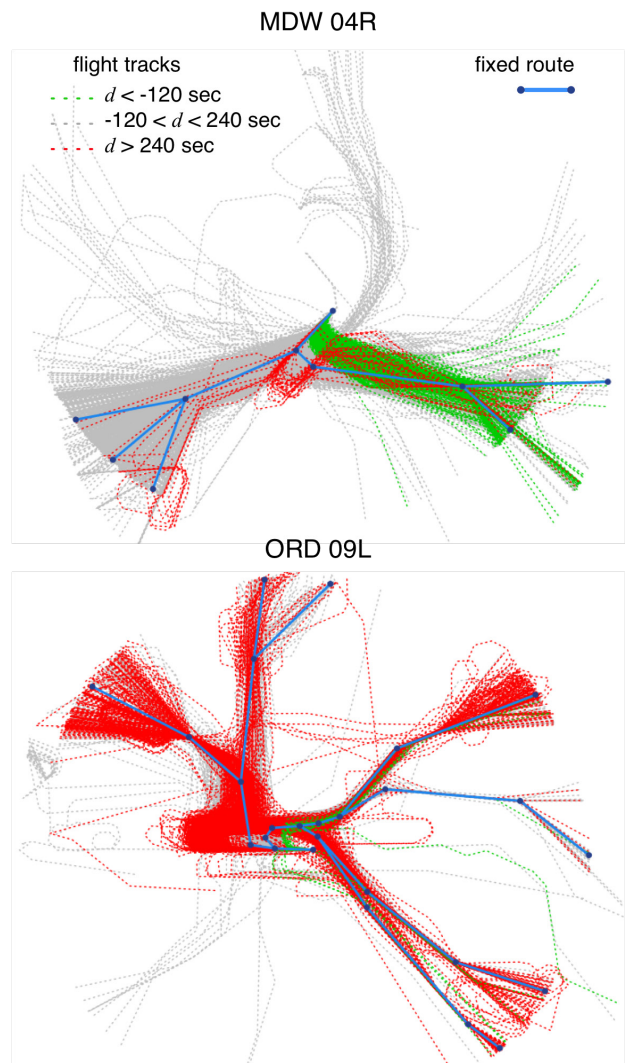


Figure 13. MDW 04R and ORD 09L Tracks

Path Stretch Delay and Time Saved by Weather Condition

Figure 14 shows 5% trimmed mean path stretch delay and time saved for $b=0.3$ nmi separated by weather condition for each runway. In general, path stretch delay and time saved are higher for IAC than VAC. The difference between the path stretch delay and time saved is scheduled delay that must be absorbed by the TRACON through speed control or passed to the center in order to keep flight on their fixed routes. Figure 15 shows an estimation of 5% trimmed mean scheduled delay by subtracting time

saved from path stretch delay by weather condition from Figure 14.

In general, there is more scheduled delay in IAC than VAC. Fast-time simulations of DEN [7] estimated the amount of delay that could be absorbed by speed control to be on the order of 2-3 minutes depending on the length of the route. Most runways in Figure 15 have scheduled delay under 2 minutes. With the exception of ATL 10, ORD 09R and 10, and LGA 22, which all have delays over 3 minutes, relatively little delay should need to be absorbed in Center airspace in order to stay on fixed routes in the TRACON.

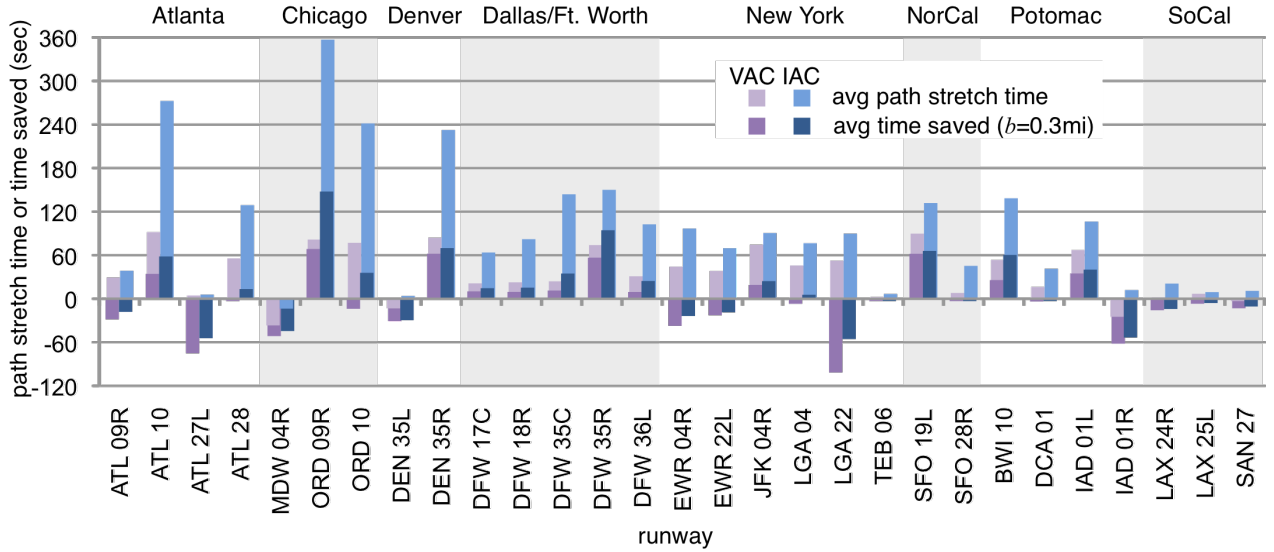


Figure 14. Path Streh Delay and Time Saved by Weather Condition

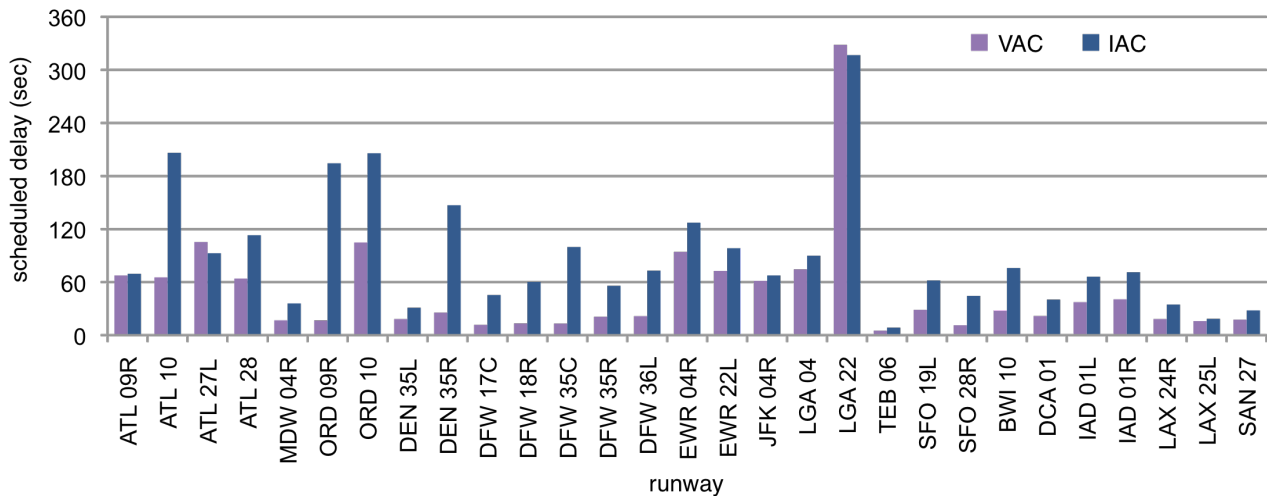


Figure 15. Scheduled Delay

Runway Interdependency Analysis

The above results are based on in-trail spacing restrictions alone. However, many runways may have other restrictions due to parallel arrival operations, shared arrival/departure operations, or crossing runways. In addition to arrival weather conditions, ASMP [18] denotes which runways were configured for arrival and departure operations per quarter hour. These data were analyzed for operations between 0600 and 2200 during the months of Feb - May 2010.

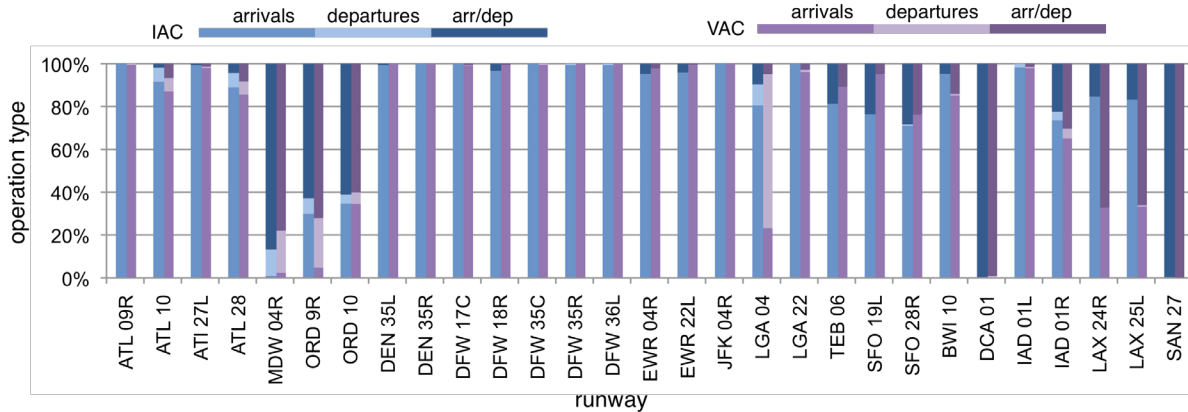


Figure 16. Shared Arrival/Departure Runway Configurations

Runways ORD 09R and 10 are shared between arrivals and departures roughly twice as often as they are dedicated for arrivals in IAC. In VAC, ORD 10 continues this trend. However, ORD 09R is hardly ever used for dedicated arrival operations in VAC, accounting for its vast difference in spacing behavior between IAC and VAC.

LAX 24R and 25L are configured for shared arrival/departure operations twice as often as dedicated arrivals in VAC only. In IAC, they are dominated by dedicated arrival operations. Runway LGA 04 is dominated by dedicated arrivals in IAC and dedicated departures in VAC with very little shared operations. All remaining runways analyzed are dominated by dedicated arrival operations in both VAC and IAC.

As can be seen in Figure 1, many of the runways analyzed cross other runways or are very close (2500 ft) to a parallel runway. Active crossing or parallel runways require coordinated operations and impose additional restrictions that affect spacing behavior.

Figure 16 shows stacked columns for IAC and VAC representing the percentage of time ASMP reported runways configured for arrivals, departures, or both in each weather state. DCA 01 and SAN 27 are always configured for shared arrival/departure operations. Other than a small percentage of time when MDW 04 is configured for dedicated departures, MDW 04 performs mostly shared arrival/departure operations as well.

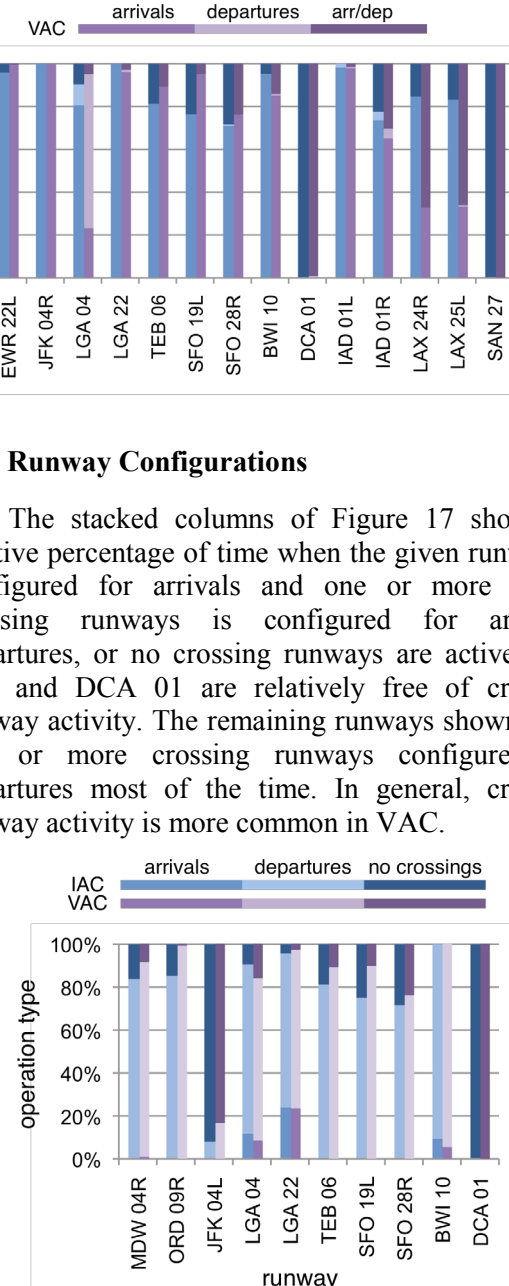


Figure 17. Crossing Runway Configurations

The stacked columns of Figure 18 show the relative percentage of time when the given runway is configured as a single arrival runway (its parallel runway is inactive) or if both parallel runways are active arrival runways.

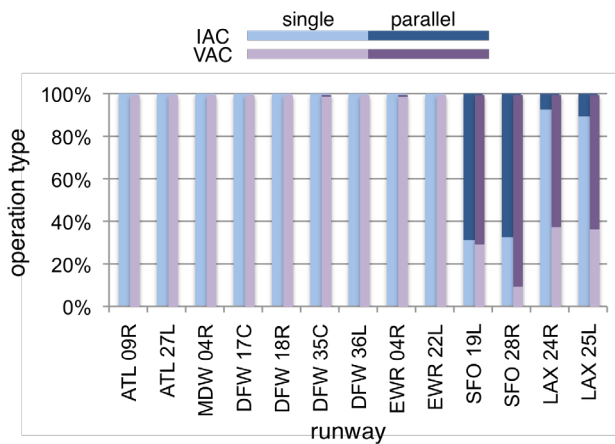


Figure 18. Parallel Runway Configurations

Only SFO and LAX runways configure both parallels for arrivals at the same time and LAX's configures both parallels for arrivals mostly in VAC. Even though SFO runways are configured for parallel arrivals most of the time in VAC and IAC, Figure 9 shows that SFO 28L is rarely ever used for arrivals in IAC. This inconsistency illustrates that the above runway configuration analysis only identifies possible (not actual) sources of procedural constraints that could affect spacing behavior. This analysis also identifies runways that are likely NOT affected by these kinds of procedural constraints because they are configured for dedicated arrival operations without active crossing or closely spaced parallel runway most of the time. These include all the runways analyzed at ATL, DEN, DFW, EWR, JFK, and IAD in VAC and IAC, as well as LAX runways in IAC only.

Conclusions

This paper discussed an analysis of spacing behavior across 29 runways from 8 top TRACONs and estimated the benefits and impacts of precision scheduling and spacing along fixed arrival routes. Likely candidate airports and runways that would benefit from precision scheduling and spacing concepts were identified. The spacing behavior and estimated capacity increases by runway suggest that

all runways analyzed would benefit from a concept that would safely allow buffers to be reduced to 0.3 nmi (at least in IAC). The analysis reinforced how different spacing behaviors can be between TRACONs, airports, and even individual runways, and that evaluations of concepts adapted to a specific site cannot be arbitrarily extended to another site.

In general, increasing separation buffers for increased required separation tend to overcompensate for the increasing standard deviations. Precision scheduling and spacing concepts would remove this unnecessary extra spacing from aircraft already widely spaced due to wake hazard and make it easier for controllers to manage these less frequently occurring aircraft pairs.

Possible procedural constraints affecting spacing due to shared arrival/departure operations, crossing runways, and closely spaced parallel approaches must be considered. Of the runways that do not appear to be affected by such procedures, reducing buffers to 0.3 nmi could increase capacity 10-20% at ATL, DEN, DFW, EWR, JFK, and LAX in IAC, and at DEN, DFW, and JFK in VAC. With the exception of LAX, all these airports have at least one runway with significant path stretch delay and could benefit from adhering to fixed arrival routing. For half of ATL and DEN runways and all DFW, and JFK runways studied, some of this delay can be reduced through precision scheduling as scheduling buffers are reduced and throughput increases. DFW and JFK runways have less than 2 minutes of scheduled delay, which may be absorbed in the TRACON with speed control. ATL 10 and DEN 35R have higher scheduled delays and so they would likely need to pass 1-2 minutes of this delay to the center.

Having identified likely candidate airports and runways that would benefit from precision scheduling and spacing concepts, the next step should be to conduct more detailed analyses and simulations on these runways. A significant number of runways with possible procedural constraints such as shared arrival/departure operations and active crossing or closely spaced parallel runways showed potential benefits. This suggests future research is needed for integration and evaluation of precision arrival scheduling and spacing concepts with these procedures.

References

- [1] Thipphavong, J., D. Mulfinger, 2010, Design Considerations for a New Terminal Area Arrival Scheduler, 10th AIAA Aviation Technology, Integration and Operations Conference, Fort Worth, Texas.
- [2] Barmore, B. E., T. S. Abbott, W. R. Capron, B. T. Baxley, 2008, Simulation Results for Airborne Precision Spacing along Continuous Descent Arrivals, 8th AIAA Aviation Technology, Integration and Operations Conference, Anchorage, Alaska.
- [3] Wieland, F., M. Santos, W. Krueger, V. E. Houston, 2011, Performance of Airborne Precision Spacing Under Realistic Weather Conditions, 30th Digital Avionics System Conference, Seattle, Washington.
- [4] Haraldsdottir, A., J. Scharl, M. Berge, E. Schoemig, M. Coats, 2007, Arrival Management with Required Navigation Performance and 3D Paths, 7th USA/Europe Air Traffic Management R&D Seminar, Barcelona, Spain.
- [5] Haraldsdottir, A., J. Scharl, J. King, E. G. Schoemig, M. Berge, 2008, Analysis of Arrival Management Performance with Aircraft Required Time of Arrival Capabilities, 26th International Congress of the Aeronautical Sciences, Anchorage, Alaska.
- [6] Haraldsdottir, A., J. Scharl, J. King, M. Berge, 2009, Arrival Management Architecture and Performance Analysis with Advanced Automation and Avionics Capabilities, 9th AIAA Aviation Technology, Integration and Operations Conference, Hilton Head, South Carolina.
- [7] Haraldsdottir, A., J. King, J. Scharl, 2010, Terminal Area Arrival Management Concepts Using Tactical Merge Management Techniques, 29th Digital Avionics System Conference, Salt Lake City, Utah.
- [8] Swenson, H. N., J. Thipphavong, A. Sadovsky, L. Chen, C. Sullivan, L. Martin, 2011, Design and Evaluation of the Terminal Area Precision Scheduling and Spacing System, 9th USA/Europe Air Traffic Management R&D Seminar, Berlin, Germany.
- [9] Thipphavong, J., H. Swenson, L. Martin, P. Lin, J. Nguyen, 2012, Evaluation of the Terminal Precision Scheduling and Spacing System for Near-Term NAS Application, 1st International Conference on Human Factors in Transportation, San Francisco, California.
- [10] Ballin, M., H. Erzberger, 1998, Potential Benefits of Terminal Airspace Traffic Automation for Arrivals, Vol. 21, No. 6, Journal of Guidance, Control, and Dynamics.
- [11] Yoon, Y., M. Hansen, 2007, The Impact of Advanced Technology on Next Generation Air Transportation: A Case Study of Required Navigation Performance (RNP), AIAA Modeling and Simulation Technologies Conference and Exhibit, Hilton Head, South Carolina.
- [12] Muller, D., P. Uday, K. B. Marais, 2011, Evaluation of the Potential Environmental Benefits of RNAV/RNP Arrival Procedures, 11th AIAA Aviation Technology, Integration and Operations Conference, Virginia Beach, Virginia.
- [13] Robinson III, J.E., M. Kamgarpour, 2010, Benefits of Continuous Descent Operations in High-Density Terminal Airspace Under Scheduling Constraints, 10th AIAA Aviation Technology, Integration and Operations Conference, Fort Worth, Texas.
- [14] Robinson III, J.E., O. Diallo, R.J. Reisman, 2011, Comparison of Trajectory Synthesis Algorithms for Monitoring Final Approach Compression, 11th AIAA Aviation Technology, Integration and Operations Conference, Virginia Beach, Virginia.
- [15] Federal Aviation Administration, 2010, 2011-2015 National Plan of Integrated Airport Systems Report, <http://aspm.faa.gov>.
- [16] Federal Aviation Administration, 2012, Air Traffic Control FAA Order JO 7110.65U Chapter 5. Section 5. Radar Separation, <http://www.faa.gov>.
- [17] Federal Aviation Administration, 2011, Air Traffic Control FAA Order JO 7110.567 Interim Procedures for Airbus A388 Flights, <http://www.faa.gov>.

[18] Federal Aviation Administration, 2012, Aviation System Performance Metrics (ASPM) Airport Efficiency, <http://aspm.faa.gov>.

[19] Koch, R., C. Treakle, R. Denmark, C. Estada, A Olsen, A. Nossaman, 2010, FAA Needs to Implement More Efficient Performance-Based Navigation Procedures and Clarify the Role of the Third Parties, Federal Aviation Administration Report AV-2011-025.

[20] Zelinski, S., 2012, A Graph-Based Approach to Defining Nominal Terminal Routing, 31st Digital

Avionics System Conference, Williamsburg, Virginia.

Email Address

Shannon.J.Zelinski@nasa.gov

31st Digital Avionics Systems Conference

October 14-18, 2012